University of Texas at El Paso
ScholarWorks@UTEP

Open Access Theses & Dissertations

2020-01-01

Development Of A Cold Gas Propulsion System For A 1u Cube Satellite

Norma Alicia Perea
University of Texas at El Paso

Follow this and additional works at: https://scholarworks.utep.edu/open_etd

 Part of the Aerospace Engineering Commons

Recommended Citation

Perea, Norma Alicia, "Development Of A Cold Gas Propulsion System For A 1u Cube Satellite" (2020). *Open Access Theses & Dissertations*. 3115.
https://scholarworks.utep.edu/open_etd/3115

This is brought to you for free and open access by ScholarWorks@UTEP. It has been accepted for inclusion in Open Access Theses & Dissertations by an authorized administrator of ScholarWorks@UTEP. For more information, please contact lweber@utep.edu.

DEVELOPMENT OF A COLD GAS PROPULSION SYSTEM FOR

A 1U CUBE SATELLITE

NORMA ALICIA PEREA

Master's Program in Mechanical Engineering

APPROVED:

Ahsan Choudhuri, Ph.D., Chair

Joel Quintana, Ph.D., Co-Chair

Rene Contreras, Ph.D.

Stephen L. Crites, Jr., Ph.D.
Dean of the Graduate School

Copyright ©

by

Norma Perea

2020

Dedication

The hard work and late hours dedicated to this project are dedicated to my parents whose great sacrifices have made me into the woman I am today. Thank you.

DEVELOPMENT AND TESTING OF A COLD GAS PROPULSION SYSTEM FOR A 1U CUBE-SATELLITE

by

NORMA ALICIA PEREA, BS

THESIS

Presented to the Faculty of the Graduate School of

The University of Texas at El Paso

in Partial Fulfillment

of the Requirements

for the Degree of

MASTER OF SCIENCE

Department of Mechanical Engineering

THE UNIVERSITY OF TEXAS AT EL PASO

August 2020

Acknowledgements

The material is based upon work supported by the National Aeronautics and Space Administration (NASA) (Grant NNX158Q04A).

Abstract

In efforts to further the development test capabilities of nanosatellites on earth, NASA White Sands Test Facility (WSTF) is developing a Magnetic Levitation Table (MLT) for ground testing of nanosatellites. Testing of the table requires dedicated test articles that employ space-like systems, but those that can be used in the confines of a small lab testing area. In collaboration with WSTF, the University of Texas at El Paso (UTEP) Center for Aerospace Exploration Technology Research (cSETR) is developing an 1U cold gas propulsion cube-satellite demonstrator (CGD) to test capabilities of the levitation table. A 1U cube satellite was designed with a cold gas propulsion system. The cold gas demonstrator, weighing 1.5kg, uses cold gas thruster configuration. The CGD uses refrigerant R-134a as the propellant as it is stored in liquid state requiring a lower fill pressure and maximizes the propellant quantity. Four thrusters are placed to provide uniaxial translation around the x-axis and rotation about the y-axis. Movement of the CGD is controlled by throttling miniature solenoid valves that feed directly to the thrusters. This work outlines the development of an integrated, self-contained propulsion unit dedicated for use as a ground-based attitude control test bed demonstrator.

Table of Contents

List of Tables

List of Figures

Chapter 1: Introduction

Interest in nanosatellites by university research institutions has grown in the last decade as technologies have evolved in favor of miniaturization of space technologies. Beginning in 1999 Stanford University and Cal-Poly have been working to develop the cube satellite standard. This standard provides uniformity in mission planning, which in-turn accelerates the program development schedule while lowering the overall cost when comparing to traditional satellite missions [1]. Growth in popularity of nanosatellites can be attributed to the low-cost nature of this platform [2]. Over 188 nanosatellites have launched in 2019 and over 450 were announced to launch by the end of 2020 [3]. Nano-satellite configurations include CubeSats, ThinSats and picosatellites, with CubeSats being the most common configuration used [4]. A CubeSat, as the name suggest, is a cube shaped satellite with standard unit (U) size of 10cmx10cmx10xm [5].

Since the completion of Cal-Poly's first successful nano-satellite mission, thousands of nanosatellites have launched into space for purposes including remote sensing, earth observation, telecommunication, and interplanetary research [4][5]. Current CubeSat designs rarely incorporate propulsion systems for orbit changing or attitude control, instead these missions favor the smaller and simpler magnetorquer systems [6]. Increasing demand for nanosatellites urges the development of these technologies to meet market requirements, particularly in the field of small-scale propulsion systems [5]. Part of the hesitation to use propulsion systems for attitude control is the lack of ground testing options. Strenuous component verification is needed for flight readiness of Cube satellites. In efforts to continue the development and testing of nanosatellites on earth, NASA White Sands Test Facility (WSTF) is developing a Magnetic Levitation Table (MLT) for ground testing of nanosatellites. NASA's MLT uses magnetic forces to levitate nanosatellite

related test articles and simulate space-like conditions within a vacuum chamber [8]. Testing of the table requires dedicated test articles that employ space-like systems, but those that can be used in the confines of a small lab testing area. In collaboration with WSTF, the University of Texas at El Paso (UTEP) Center for Aerospace Exploration Technology Research (cSETR) is developing an 1U cold gas propulsion cube-satellite demonstrator (CGD) to test capabilities of the levitation table. This work outlines the development of an integrated, self-contained propulsion unit dedicated for use as a ground-based attitude control test bed demonstrator.

Chapter 2: Background

To assist in the development of the MLT, a 1U cube satellite was designed with a cold gas propulsion system. The satellite, referred to as a cold gas demonstrator (CGD) is designed to Cal-Poly's CubeSat Design Specifications [9]. The cold gas demonstrator, weighing 1.5kg, uses cold gas thruster configuration. Cold gas system is used on the demonstrator to maintain simplicity and safety. Cold gas systems offer the added value of having few developmental obstacles, making it optimal for academic use. The CGD uses refrigerant R-134a as the propellant as it is stored in liquid state requiring a lower fill pressure and maximizes the propellant quantity. Four thrusters are placed to provide uniaxial translation around the x-axis and rotation about the y-axis. The design has been constrained for testing operations on a 20-inch by 10-inch levitation table. Movement of the CGD is controlled by throttling miniature solenoid valves that feed directly to the thrusters. The translation and rotation of the CGD is measured and controlled using an Inertial Measurement Unit (IMU) signaling the Onboard Computer (OBC) and electrical controls which directly power the engine.

SECTION 2.1: PROPULSION SYSTEM DESIGN AND ARCHITECTURE

Traditional cold gas propulsion systems are simple consisting of a propellant storage tank, a fluid control valve and nozzle, as seen in Figure 2.1 [6]. While no nanosatellite propulsion systems are commercially available at the present moment, proposed small satellite propulsion systems are single-nozzle devices designed for translational maneuvers [10]. Cold gas engines generate thrust through the expansion of a propellant gas as it flows into the nozzle and out to the atmosphere [4]. Although cold gas thrusters are considered the simplest and most reliable propulsion systems, they offer relatively low specific impulse [7] and are not propellant efficient.

Cold gas thrust is dependent on the propellant atomic mass [4]. However, as attitude control applications generally require only low thrust levels, a cold gas system was ideal for this project.

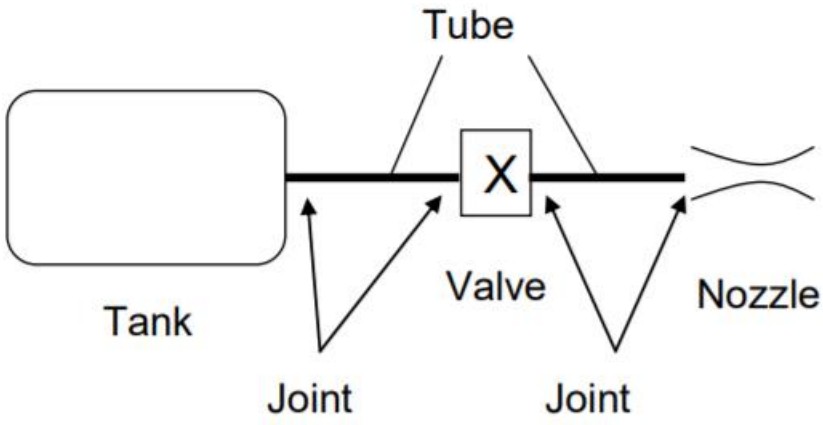

Figure 2.1: Basic Cold Gas Propulsion System [6]

SECTION 2.2: COLD GAS PROPULSION SYSTEM

Cold gas propulsion systems offer a low total impulse ($\Delta V < 50$ m/s), with overall performance dependent on the nozzle inlet stagnation pressure and temperatures [7]. As the propellant is released from the propellant tank the temperature and pressure inside decrease, this is known as the Joule Thompson effect. Temperature changes during this process occur when a flowing gas passes through a pressure regulator, throttling device, or valve. The cooling process in a cold gas system is usually undesirable, therefore a heating element is usually integrated into the tank design to compensate for temperature changes. As system become more complex it is important to keep the pressure at the nozzle inlet consistent. This is done by heating the propellant tank to the necessary conditions, increasing the upstream pressure which is typically regulated using pressure regulators and relief valves as seen in Figure 2.2 [7].

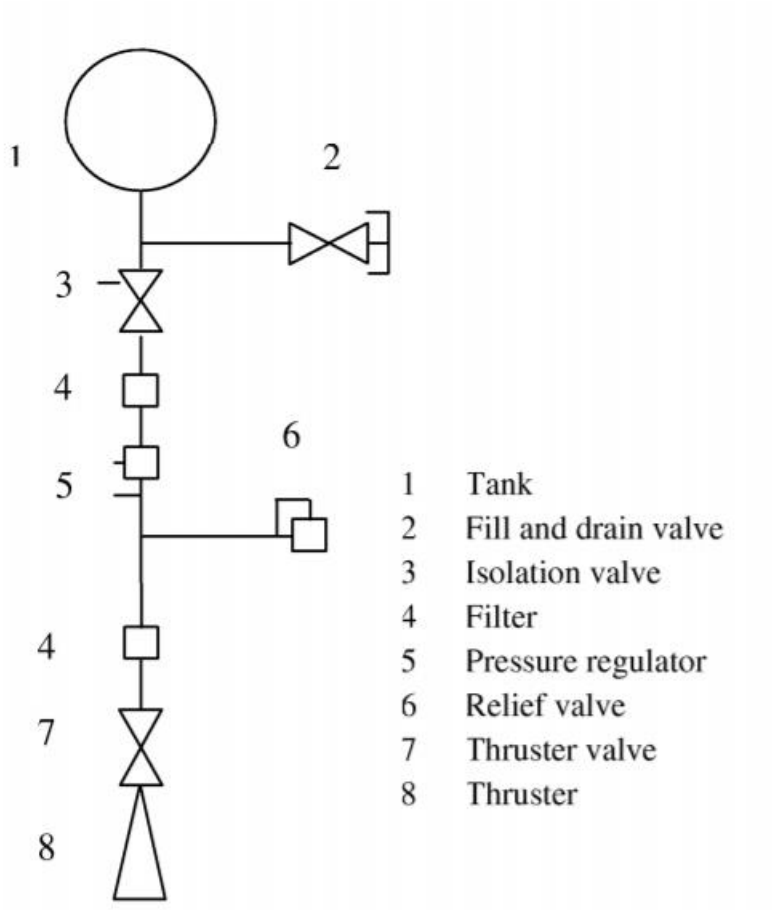

Figure 2.2: Layout of Cold Gas System [7]

The simplicity of a cold gas system requires that all feed system components be carefully selected to meet testing requirements. Feed system components can be tested individually to characterize flow performance and response time. This maximizes the overall performance of the cold gas system. Although, manufacturers often provide information regarding component performance, some feed system components have unique characteristics that require strenuous testing and verification of flow performance. In addition, the propellant chosen is critical to system performance. Various propellants were analyzed for use onboard the CGD including Nitrogen gas, Helium gas, Argon gas and Refrigerant 134a. Refrigerant 134a is used for the CGD's propellant based on its high storage density in the liquid state. Combined with a low toxicity level, R-134a

maintains a high level of safety for use in an enclosed laboratory space. NASA's safety guidelines require that pressurized system not be higher than 400psig for small satellite projects. The refrigerant can be stored at low pressures (between 50-100psig) and raised to a working pressure of 150psig using heating elements integrated into the propellant storage tank design.

SECTION 2.3: DESIGN CONCEPT

NASA's levitation table operational limits confine the size of the demonstrator to a 1U cube satellite with a maximum allowed weight of 1.5 kg. Design of the CGD consolidates the satellite chassis and propellant tank. The primary purpose of integrating the chassis and the propellant tank to one component was to maximize the space taken up by the propellant tank. NASA requirements to test the MLT require a minimum of 10 minutes of continuous testing. Cylindrical and spherical pressure vessel volume distribution can be awkward to integrate into a confined space. Although unconventional, a square pressure vessel allows maximum storage of the propellant in a thin and evenly distributed space. Incorporating support structures to the interior of the tank reduce stresses of the tank. The consolidated chassis also allows ease of integration for electrical and communication components, as these components follow standard dimensions.

Flow to the thrusters is controlled by a miniature manifold valve at the tank and at each inlet of each thruster. Four thrusters are evenly placed on two opposing faces of the chassis. Prior to operating the thrusters, R-134a is heated to appropriate pressures and temperatures. The pressurized gas is controlled by an isolation valve that controls the flow of propellant to the engine. Pressure drops through the miniature solenoid valves are compensated to maintain optimal flow conditions within the thruster. Operation of two thrusters simultaneously gives lateral translation in the x-axis and rotation along the z-axis.

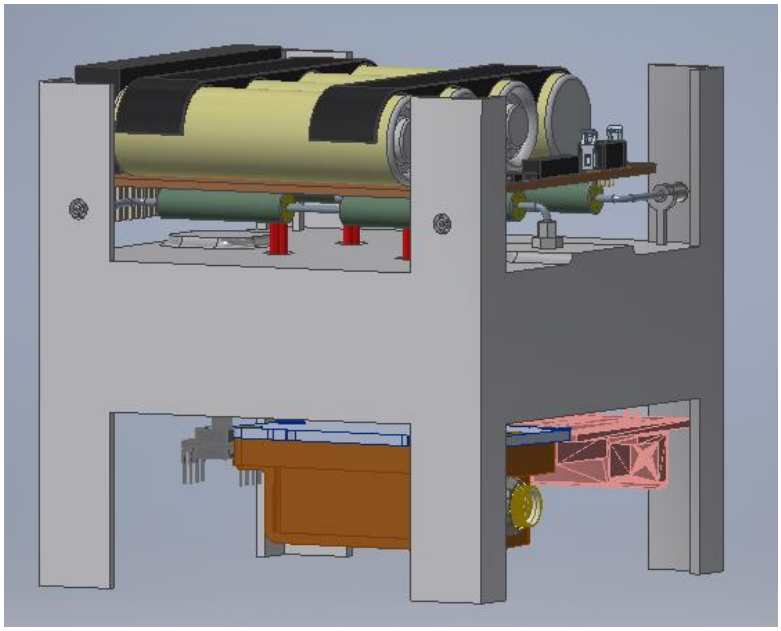

Figure 2.3: Cold Gas Demonstrator Module Conceptual Design

The integrated satellite includes propellant storage and feed system, four independently operated thrusters, telemetry sensors, thermal control system, inertial measurement unit (IMU), wireless communications, and self-contained avionics. The complete integrated module is shown in Figure 2.3.

Chapter 3: System Components

SECTION 3.1: MINIATURE SOLENOID VALVE

Fluid control from the tank to the thrusters is done using a miniature solenoid valve developed by the Lee Company, seen below in figures 3.1 and 3.2. Being a new product available in the market, the manufacturer information of the performance of the solenoid valve, referenced as MSFC-SOV in this paper, is scares. The valve requires spike and hold voltages to pull the internal mechanisms allowing flow through the valve. According to Camacho et. Al., the miniature solenoid valves require a microcontroller (MSP) and specialized electrical system control the valve, supplying 24V for 3.3ms then dropping to a hold voltage of 3.8V. Miniature electrical components are often delicate and experience noise from external power sources, these fluctuations in signal may affect the functionality of the miniature solenoid valve. The distortion in signal can cause the valve to fail to open fully, creating an obstruction in the flow to the thrusters or may cause the valve to over-heat causing an electrical short.

Figure 3.1: LeeCo Miniature Solenoid Valve

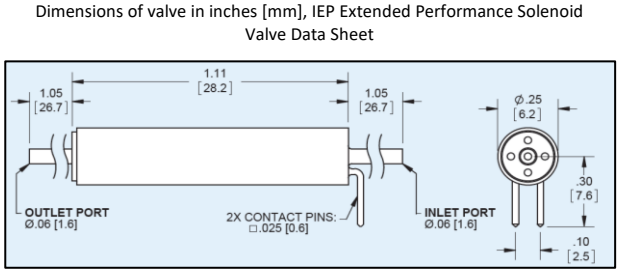

Figure 3.2: LeeCo Miniature Solenoid Valve Schematic

Figure 3.3 demonstrates an analysis done my Camacho et. Al. to determine the maximum allowed current supplied to the solenoid valve without damage to internal mechanisms while

allowing the valve to open fully. The analysis found that at reducing the input current to 63.2% continued to allow the valve to have full functionality [8].

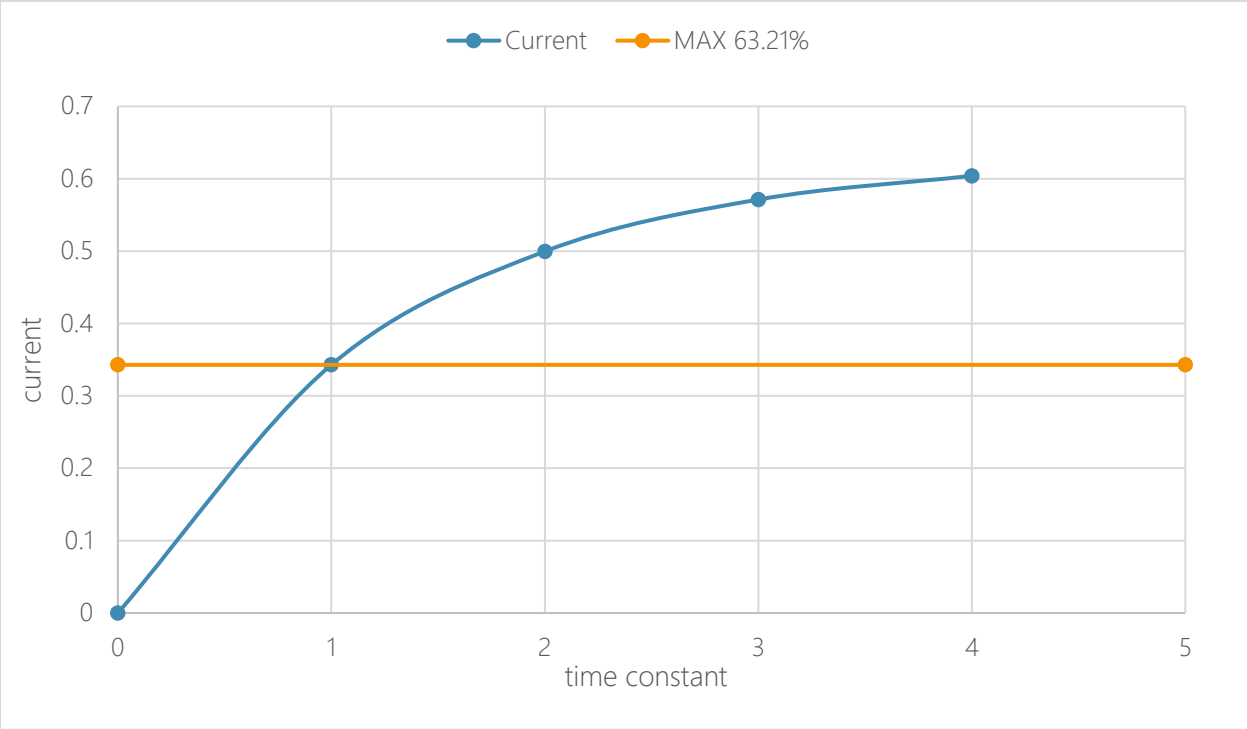

Figure 3.3: Valve Current Analysis [8]

3.1.1 Valve Characterization

The relationship flow rate and pressure drop rate of a valve can be expressed by equation 3.1 below. Where K is the valve flow coefficient, pressure drop across the valve is ΔP, the exit pressure and temperatures are P_2 and T_2 respectively, and SG is flow specific gravity [7].

$$Q = K_v \sqrt{\frac{293\ \Delta P P_2}{SG\ T_2}} \tag{3.1}$$

In addition to characterizing the appropriate power requirements needed to throttle the MSFC-SOV, valve properties such as pressure drop, response time and exit flowrate are characterized using gaseous nitrogen (GN2) as per Camacho et al [8]. Valve characterization includes a series of 60 GN2 cold flow tests to measure the pressure drop across MSFC-SOV and 56 tests to measure the response time of the system. Each test is implemented using 50% duty cycle with 20-second pulses [8] results from this testing can be seen in Table 3.1.

Table 3.1: Pressure drop and response time measurement for preliminary tests [8]

TESTING PRESURE	INLET PRESSURE psi	OUTLET PRESURE psi	ΔP psi	RISE TIME sec	FALL TIME sec	Flow Rate (SLPM)
100±10	96.8	90.3	6.5	3.3	3.5	4.28
110±10	109.9	102.0	7.8	2.3	3.4	5.13
120±10	120.2	111.3	9.0	3.5	4.0	5.87
130±10	130.0	120.0	10.0	3.6	4.0	6.39
140±10	140.6	129.4	11.2	3.6	3.6	6.97
150±10	150.3	138.0	12.3	3.0	4.1	7.55
160±10	160.2	146.7	13.5	3.2	3.5	8.12
170±10	171.0	156.1	14.8	3.1	3.7	8.77
180±10	181.1	165.0	16.1	3.6	3.6	9.32
190±10	190.6	173.2	17.4	2.9	3.7	9.85
200±10	200.0	181.2	18.8	3.6	3.9	10.41

Table 3.1 demonstrates the average pressure drop across the solenoid valve flowing nitrogen gas and a pressure range of 100 psig-200 psig with increments of 10 psig. The response time of the system has an average rise time of 3.2 seconds and fall time of 3.7 seconds.

Following GN2 cold flow testing, the same response time and pressure drop tests are done using R-134a as the working fluid. Figures 3.4 demonstrate the pressure drop measurements using R-134a across the miniature solenoid valve for inlet pressures of 120 psig and 110 psig respectively. These test results are data points gathered during the preliminary tests done on the system using R-134a. These graphs indicate the measured pressure drop across the miniature solenoid valves to range from 30-40 psig. Such a high-pressure drop is attributed to the high

density of the refrigerant as well as unexpected cooling on the refrigerant across the delivery line. Since the refrigerant is heated and insulated up stream of the solenoid valve, it was found that allowing the refrigerant to sit idle in the delivery line could cause it to cool down at which point the refrigerant would be a saturated mixture opposed to the expected gas.

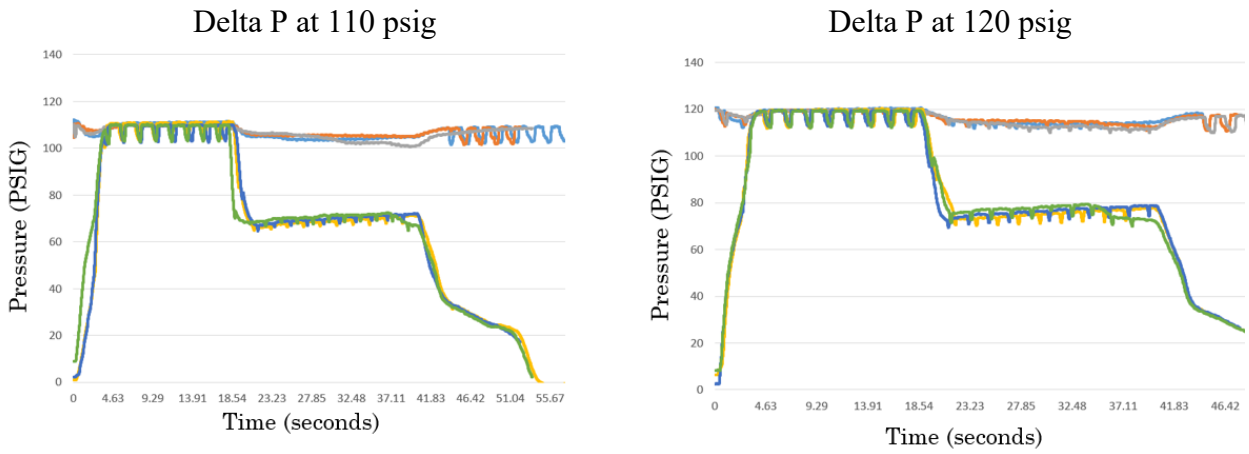

- **Note:** Tank pressure will be set to 140 psig to compensate for pressure drop across valve, this is to set thruster pressure chamber at 100 psig

Figure 3.4: R-134a Pressure drop and response time measurement at 110 PSIG

A second series of test were conducted using refrigerant, the results are seen on table 3.2. These results show a pressure drop of 30.7-51.15 psig this high pressure drop across the solenoid valve can be attributed to the environmental conditions of the testing facility. The environmental conditions during the preliminary test revealed the requirement of the entire feed system to be insulated to reduce heat losses to the cold environment of the test facility. Colder testing environments require the feed lines to be pre-heated to reduce condensation of the refrigerant as it flows downstream. The second test matrix was conducted in higher temperature setting requiring only the high-pressure side of the feed system to be heated and insulated.

Table 3.2: Pressure drop and response time measurement for R-134a

Test Pressure (PSIG)	Inlet Pressure (PSIG)	Outlet Pressure (PSIG)	Delta P (PSIG)	Response Time (seconds)
110	95.12	66.9	28.23	2.44
110	102.27	71.5	30.77	2.93
120	113.6	74.9	38.7	3.27
130	126.3	85.6	40.43	3.41
140	134.4	93.5	40.9	4.11
150	143.7	90.9	52.8	3.0
160	157.3	99.2	52.07	3.29
170	161.9	110.8	51.15	3.8

SECTION 3.2 TESTING FACILITY

A delivery system was designed for thrust verification testing of the CGD engine, the test set-up is located at UTEP cSETR's Fabens test sight. The testing facility used for these test campaigns is composed of several regions: A propellant feed line composed of two gas inlet lines joined to a singular feed line. A recapturing system to control the release of R-134a to the atmosphere. A torsional thrust stand system with laser displacement measurements and data acquisition system for all electrical equipment, as seen in Figure 3.5 and 3.6. The test facility is intended to have multifunction capabilities for ease of experimentation between the miniature solenoid valves and thrust verification testing of the cold gas nozzle. The delivery feed lines lead to the test article sight. Modifications for thrust measurement testing are minimal and include only the installation of the cold gas nozzle onto the torsional thrust stand and installation of laser measurement devices.

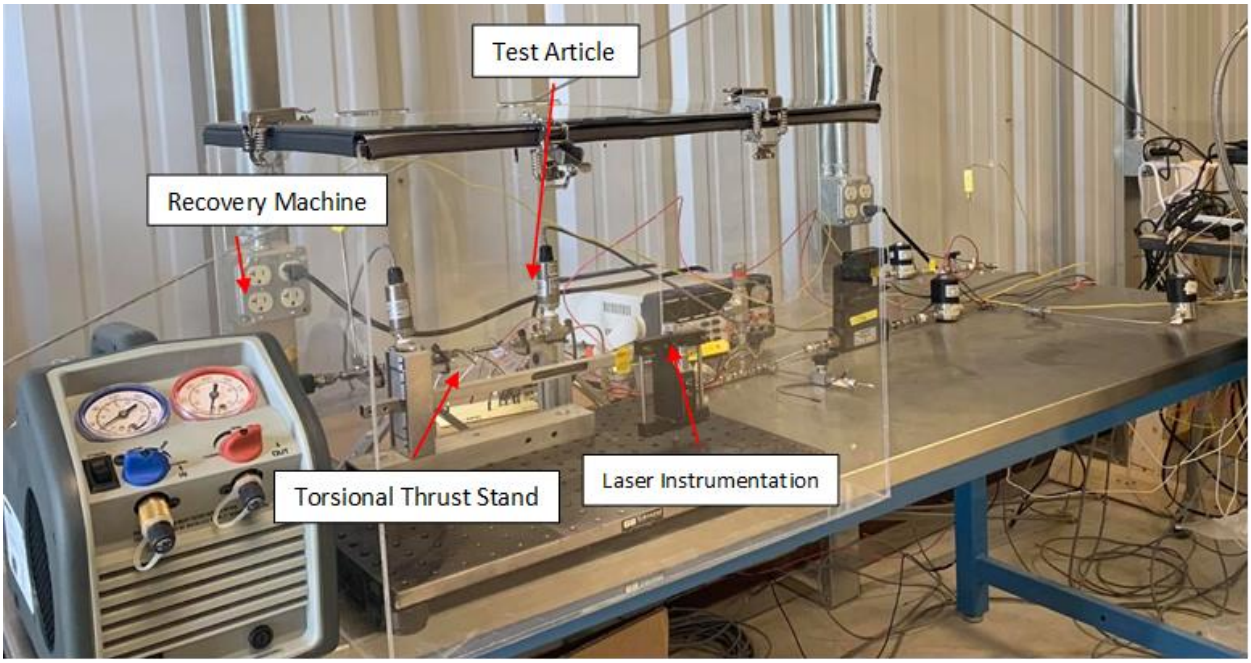

Figure 3.5: Thruster Testing Delivery System

Feedline System

Test facility fluid delivery feed lines are outfitted with solenoid and hand valves for fluid control; flow meters, thermocouples, throttling valves, and pressure transducers for adjusting and monitoring fluids. To ensure proper data collection from electrical instrumentation, all data acquiring components are calibrated before installation to the delivery feed line. Data measurements devices should be re-calibrated through the manufacturer every two years to ensure proper results during testing.

Due to the environmental risks of flowing refrigerant R-134a into the atmosphere, a recapturing system encapsulates the torsional thrust stand to control the release of R-134a. Refrigerant 134a has been found by the EPA to an ozone depletant, there for release of refrigerant into the atmosphere is greatly discouraged. Release of refrigerant is limited to *de minimis,* meaning that 'good faith' attempts to recapture and recycle or safely dispose of refrigerant must be made, limiting the release of refrigerant to releases that occur when connecting or disconnecting hoses to

charge or service appliance. The recapturing system design includes an acrylic box enclosure with sealed inlet and outlet ports, to prevent exhaust of refrigerant gases. The acrylic enclosure connects to a refrigerant recovery machine capable. The recovery machine works by cooling the refrigerant gas to a condensed state. The liquid refrigerant is then pumped into a recovery tank were the used refrigerant can be stored and safely disposed. Figure 3.6 below denotes the piping and instrumentation diagram for the test facility.

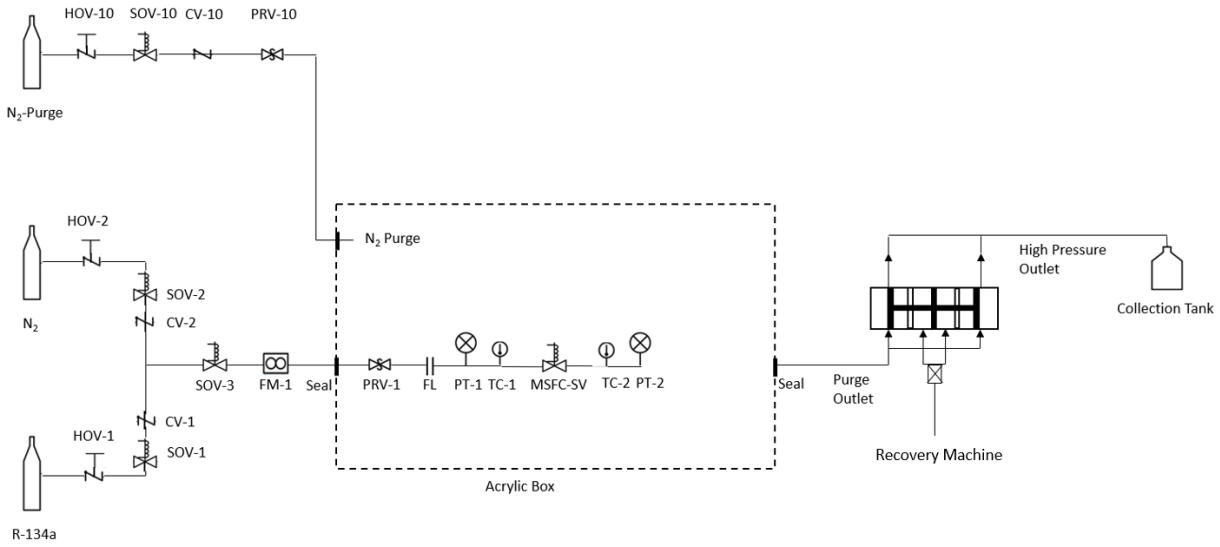

Figure 3.6: Test Setup Piping and Instrumentation Diagram

Thruster testing is initiated by pressurizing the source tank to 200 psig at 160 C using specialized refrigerant tank heating sleeves. The heating sleeve apply low heat to the base of the source tank as to prevent sudden over pressurization of the tank. The heating sleeve is equipped with internal temperature sensors controlling the voltage intake to the heating sleeve; this maintains the heating sleeve at 175 °C, raising the internal temperature of the tank to 160 °C. Redundant sensor controls were placed on the high-pressure side of the system so that the tank would not over-heat or over pressurize. This was done by placing thermocouples on the tank walls

and upstream of the refrigerant delivery line. A pressure relief valve set to 200psig prevents over-pressurization of the source tank while a pressure gauge on the refrigerant delivery line feeds a constant pressure to the thruster.

LabView Data Acquisition System

All electrical components included in the test facility are commanded using National Instruments LabView 2020 Software. A user interface was developed to control the flow of nitrogen and refrigerant gasses to the test article as well as monitor fluid pressure and temperature up stream of feed line system and at the test article. The LabView interface is controlled manually by testing personnel and allows the user to communicate with the electrical system and MSP controller referenced in Camacho et. Al. The user interface provides real time measurements of fluid pressure, temperature, and mass flowrate to test personnel. The user interface is also equipped with built in red lines to signal the test personnel of potential safety concerns. In the event of over pressurization/heating of the feed line system, power to all equipment maybe shut off manually by switching off all DC power sources to the system, closing all solenoid valves and turning off heating sources. Once all power has been shut off to the system may be allowed to cool down before personnel may approach the test table to manually open exhaust valves. The MSFC-SOV is controlled by a pre-programmed MSP board which is triggered through LabView. Feed line system sensors and controls communicate with LabView using a National Instruments compact cRIO-9030, which is a high-performance embedded controller featuring I/O modules, industrial communication, and human machine interface (HMI) capabilities. The user interface and LabView program can be seen in figure 37-3.9 below.

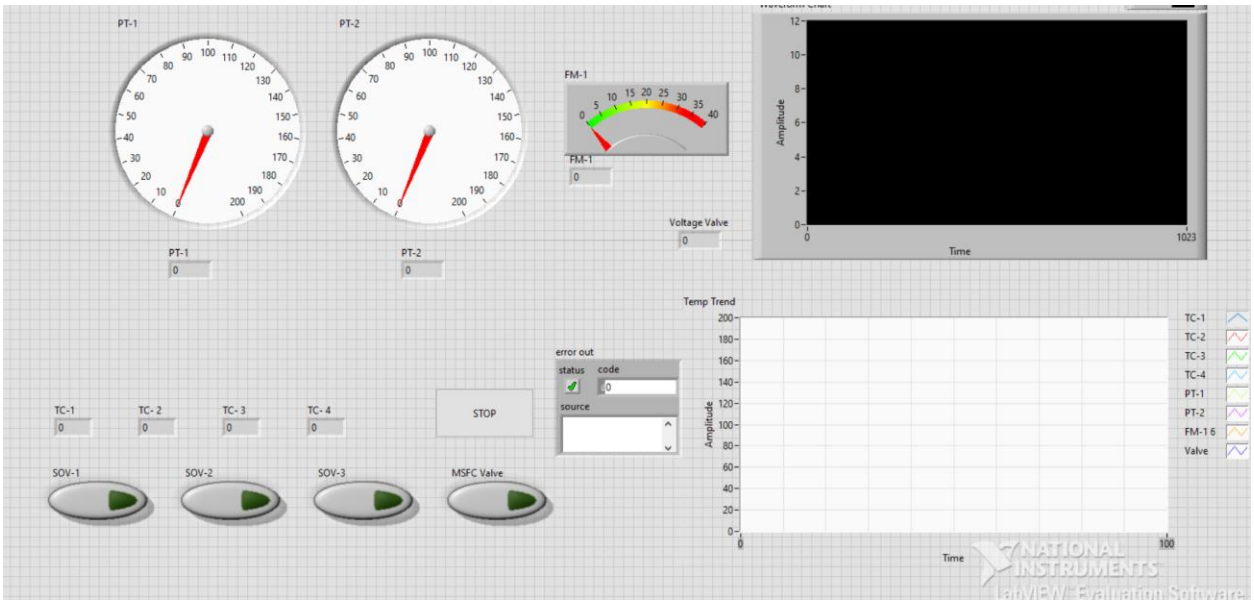

Figure 3.7: LabView User Interface

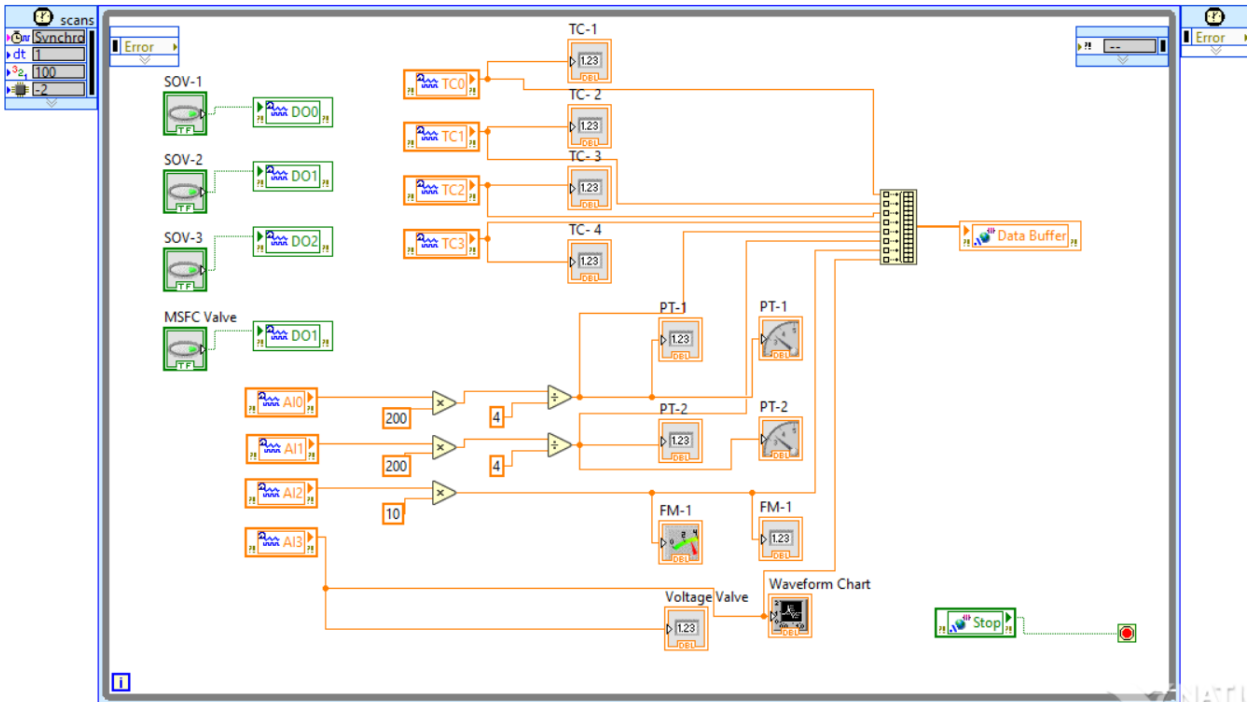

Figure 3.8: LabView Sensor Communications Code

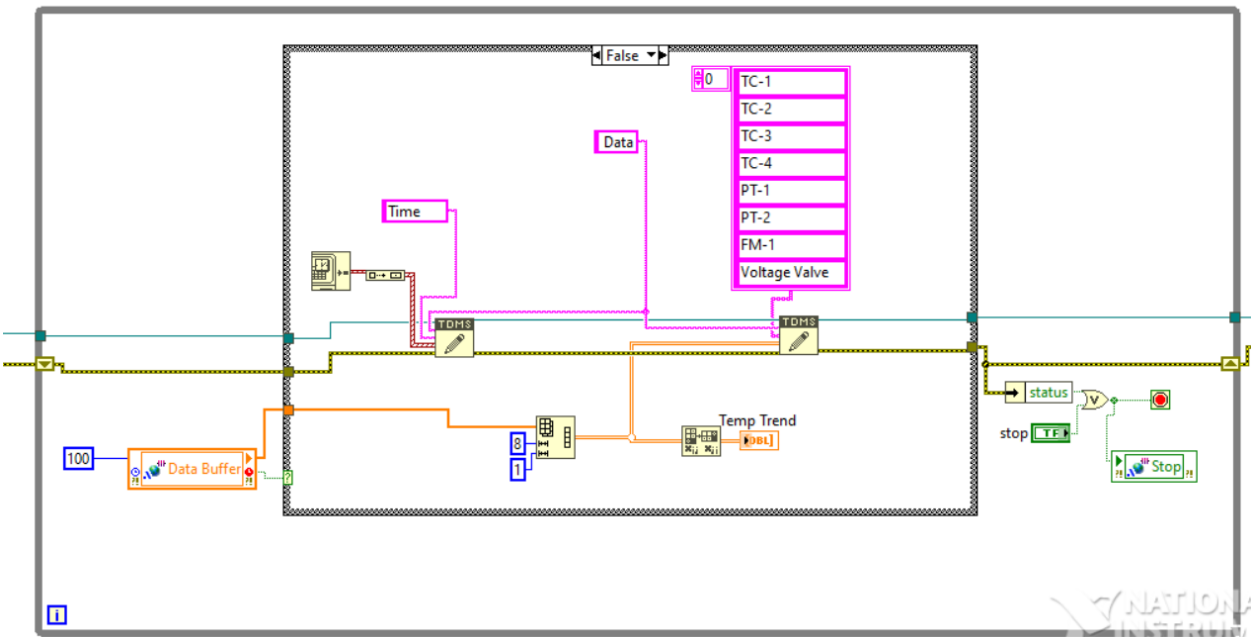

Figure 3.9: LabView Data Acquisition Code

Torsional Thrust Stand

While pipe pressure losses can be neglected, feed system components typically have a larger effect on the performance of a cold gas system. Feed system components to consider for analysis and characterization include various types of valves, filters, orifices and pressure regulators [7]. Performance of components can usually be provided by manufacturer. However, this may not be the case for all instrumentation such as prototypes. Being prototype valves, Lee Company Miniature Solenoid Valves (MSFC-SOV) used in the CGD feedline assembly, are tested to characterize the pressure drop and response time of the valve. This testing serves as an integral part of the development process to accurately measure the performance of micro-thrusters.

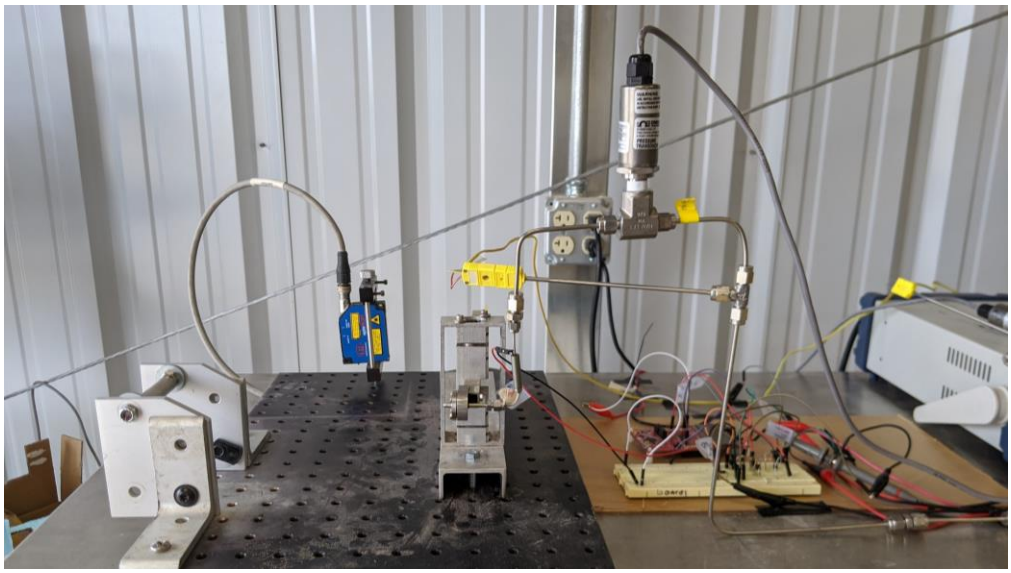

Figure 3.12: Thrust Stand and Laser Measuring System

As mentioned before, the miniature solenoid valves were fully characterized before integration to full engine assembly. A series of thrust measurement tests were done on the CGD engine. The engine in this scenario refers to a completed valve-thruster assembly, seen in figure 3.10. Thruster testing is conducted using a torsional thrust stand and laser equipment. INFICON Software records displacement of the torsional thrust stand which is measured by the laser. The data measured is then submitted into a MATLab code to calculate the thrust output. The thrust stand and laser measurement system can be seen in figure 3.11 and 3.12.

Figure 3.10: Engine Assembly

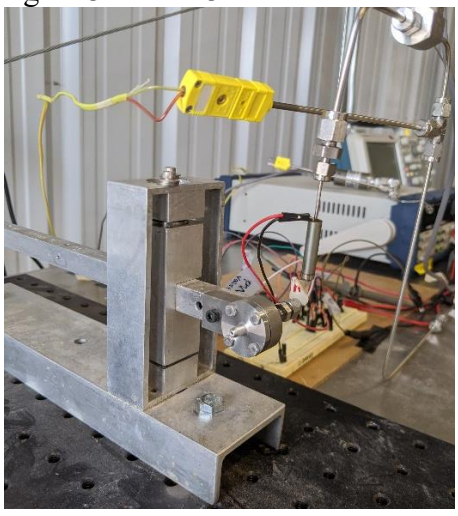

Figure 3.11: Thrust Stand Assembly

Thruster testing includes 30 calibration tests measuring a known force applied onto the torsional thrust stand and measuring the displacement of the torsional thrust stand arm. The thrust stand is calibrated with a pressurized line to acknowledge the dampening effect of the feed system line on the thrust produces. The calibration curve can be seen in figure 3.13 below.

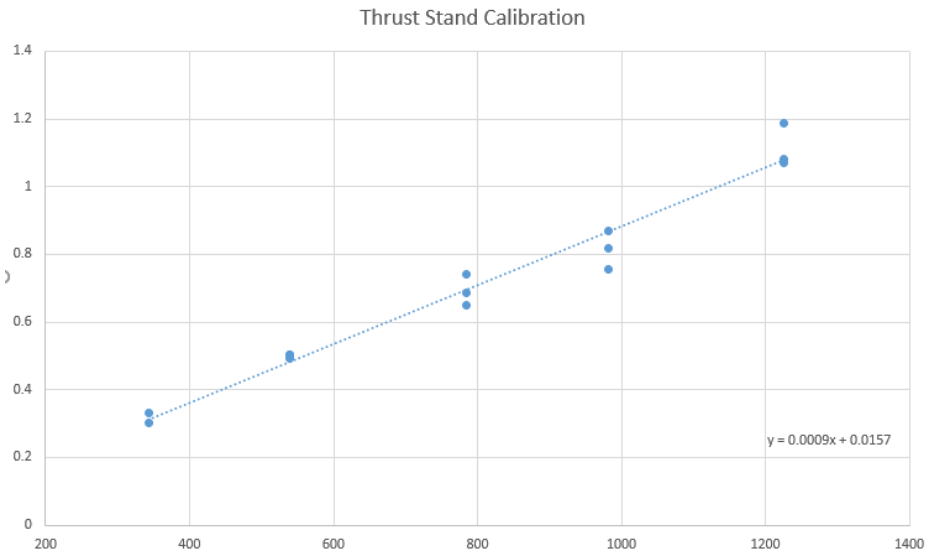

Figure 3.13: Thrust Stand Calibration

SECTION 3.3: THRUSTER DEVELOPMENT

The total estimated mass of the cube-sat including communication and electronic systems, temperature and pressure controls, fuel, and mechanical components is 1.56 kg. Based on this mass estimate a micro-thruster was developed capable of supplying a theoretical thrust of 675mN with a chamber pressure of 100 psig.

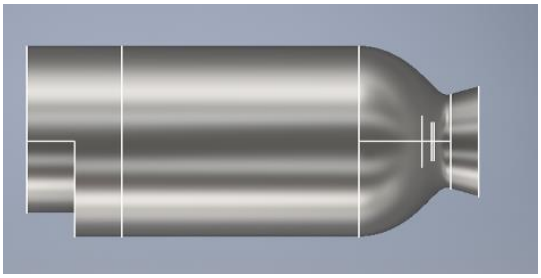

Figure 3.14: Sea Level Thruster

As mentioned previously, cold gas engines generate thrust by using the expansion of the propellant gas typically stored at high pressures. The engine on board the CGD is referred to the miniature solenoid valve and thruster assembly. The CGD stores R-134a in a liquid state. When intended to fire, R-134a will be heated to firing conditions (40 C @ 1016 kPa). The pressurized gas is controlled by an isolation valve, which then feeds the propellant to the engines. Firing conditions were selected to compensate for pressure drops along the delivery lines. Each thruster will experience a mass flow 0.0013kg/s per thruster and evaporative cooling 231.14 W.

3.2.1 Thrust Design Theory

Cold gas thrusters are simple mechanisms whose performance relies heavily on the employed solenoid valves and fluid properties to provide a consistent fluid flow to the pressure chamber. Thrust for a simple cold gas system is given by equation 3.2, where the thrust coefficient C_F can be determined using equation 3.3. P_c is the critical pressure at the chamber and A_{th} is the cross-sectional area of the nozzle throat. C_{Fi} is the ideal thrust coefficient and C_{Fv} is the viscous effect of on the thruster coefficient [7].

$$F = C_F \, P_c A_{th} \tag{3.2}$$

$$C_F = C_{Fi} - C_{Fv} \tag{3.3}$$

Performance of low thrust nozzles is highly dependent on the viscosity of the working fluid, which is affected by the nozzle's Reynolds number at the throat. Two computational models were used to validate analytical results for the thruster's throat diameter. The first model, an excel model, requires firing conditions at which the thruster is expected to perform to calculate the appropriate dimensions for the chamber and throat. This model uses the stagnation pressure and temperature at the nozzle inlet to determine the mass flow rate at the exit of the nozzle as seen in equation 3.4.

$$\dot{m}_e = C_d\sqrt{\gamma}\left(\frac{A_{th}P_c}{\sqrt{RT_c}}\right)\left(\frac{2}{\gamma+1}\right)^{\frac{\gamma+1}{2(\gamma-1)}} \tag{3.4}$$

The second model, a MATLAB model, back calculates the required pressure input and chamber dimensions pertaining to the desired throat diameter assuming isentropic flow to determine critical pressure ratio. This model uses the critical pressure and temperature to determine the mass flow rate at the nozzle exit as seen in equations 3.5-3.6. Once the mass flow rate at the desired throat diameter has been determined the mass flow rate is used to determine the thrust properties of the specified nozzle dimensions.

Isentropic Flow

$$\frac{A_e}{A_0} = \left(\frac{k+1}{2}\right)^{-\frac{k+1}{2(k-1)}}\frac{\left(1+\frac{k-1}{2}M_e^2\right)^{\frac{k+1}{2(k-1)}}}{M_e} \tag{3.5}$$

$$\frac{T_e}{T_0} = \left(1+\frac{k-1}{2}M_e^2\right)^{-1} \tag{3.6}$$

$$\frac{P_e}{P_0} = \left(1+\frac{k-1}{2}M_e^2\right)^{-\frac{k}{k-1}} \tag{3.7}$$

Choked Mass Flow Rate

$$\dot{m} = \frac{A_0 P_0}{\sqrt{T_0}} \sqrt{\frac{k}{R}} \left(\frac{k+1}{2}\right)^{-\frac{k+1}{2(k-1)}} \tag{3.8}$$

General Thrust Equation

$$F = \dot{m} V_e + (P_e - P_\infty) A_e \tag{3.9}$$

Both models are integral tools to calculate expected performance results for idealized conditions and later for modifications to thruster design based on changing requirements.

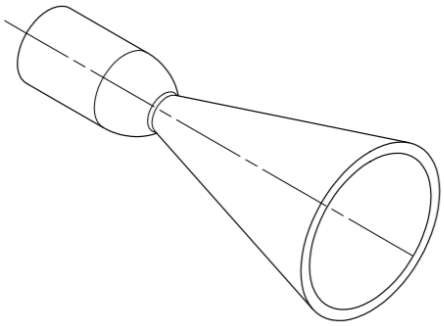

Figure 3.15: Cold Gas Nozzle Design for Vacuum Conditions

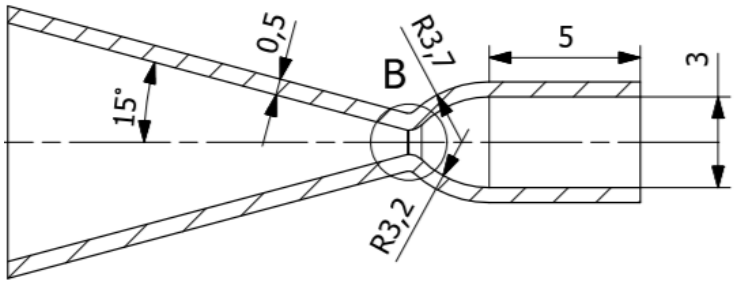

Figure 3.16: Cold Gas Nozzle Dimensions for Vacuum Conditions

Preliminary thruster design was capable of supplying 200mN of thrust. A mass budget analysis was done on the satellite, which demonstrated that 200mN of thrust would not be sufficient for MLT testing. Based on the new established requirements, various thruster dimensions were calculated and can be seen in the table 3.2 below. A conical shaped nozzle was designed based using a one-dimensional empirical model. Design of the nozzle can be seen in figure 3.15 and 3.16. Expansion of propellant gas at the exit nozzle is idealized as isentropic and flow is demonstrated to be choked using the critical pressure ratio. A correction factor of 0.9829 is applied to the thrust to account for the conical nozzle. Wall thickness of the thruster allows the pressure chamber to withstand a maximum pressure of 200 psi at a temperature of 25°C. The overall performance of the thrusters with the chosen propellant should not fall below a minimum Isp of 35s.

Table 3.3: Thruster Characteristic Analysis

d_0 (mm)	**d_e (mm)**	**Thrust (mN)**	**Evaporative Cooling (W)**	**Run Time (min)**
0.4	2.53	164	60	22
0.5	3.16	257	94	14
0.6	3.79	370	135	10
0.7	4.43	503	184	7.3
0.8	5.06	657	241	5.6
0.9	5.69	832	304	4.4
1	6.32	1030	376	3.6

Changes in testing requiremtents of the levitation table required the demostrator to include nozzle design conditions with lower expansion ration in place of idealized nozzle expansion for vacuum conditions. The thruster design was altered to include similar throat and chamber dimensions and expansion ration of 5. A plate is added to the end of the pressure chamber to allow

the thruster to be mounted onto the thrust stand adaptor as well as to function as an interface for the final assembly of the CubeSat. The preliminary design for sea-level thruster can be seen in figures 3.17 and 3.18.

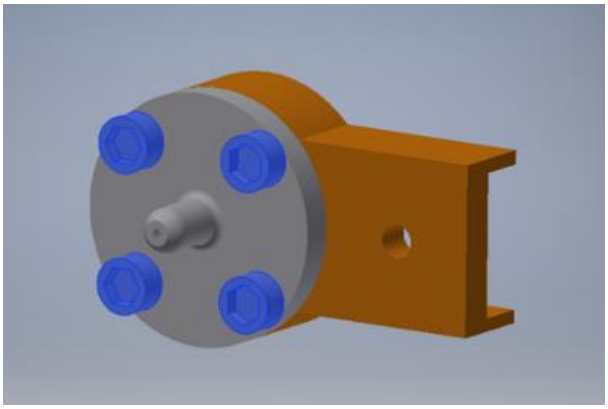

Figure 3.17: Preliminary Thruster CAD

Figure 3.18: Manufactured Thruster

The final sea-level thruster CAD and final manufactured thruster can be seen in figure 3.17 and 3.18, respectively. A specially sized mounting plate, seen attached to a micro-thruster in figure 3.19, was machined to prepare the miniature thrusters to an existing torsional thrust stand system, previously design and verified by past UTEP alumni.

Figure 3.19: Cold Gas Nozzle

The final manufactured design for the cold gas nozzle can be seen in figure 3.19. Each thruster has a theoretical thrust of 675mN at nozzle inlet properties of 25°C and 690 kPa. Performance calculations of the thruster were done considering ideal testing conditions with nozzle inlet temperature at room temperature conditions. Table 3.3, bellow denotes theoretical performance of the cold gas nozzle at three inlet temperature cases. The first being ideal testing conditions with the propellant inlet temperature of 25°C. The second being the propellant properties expected from heating the CGD pressure vessel to 160°C. The third case considers heat losses from the propellant source tank to the nozzle inlet during testing in laboratory environments with a nozzle inlet temperature of 41°C. Performance calculations can be seen in Appendix A.

Table 3.4: Analyzed Thruster Characteristics

	Ideal Propellant Conditions	CGD Heated Propellant Conditions	Laboratory Testing Conditions
Chamber Temperature (K)	298	344	283
Propellant Saturation Pressure (kPa)	690	2169	488
Propellant Flow Rate (kg/s)	0.0013	.0012	1.4
Nozzle Exit Velocity (m/s)	367	394	305
Nozzle Exit Temperature (K)	217	250	225
Thrust (mN)	673	610	493

3.2.3 Testing and Results

Thrust varification testing of the cold gas nozzle measured the force output by two sea-level thrusters. A series of twelve tests were conducted with an inlet nozzle pressure of 100 psig. Testing also included measurement of system response time. Each test is implemented using 50% duty cycle with 5-second pulses results from this testing can be seen below in figure 3.20. Data measurement points are filtered using Fast Furrier Filter (FTT) and further refined using Gaussian Kernel Density Function. The results from the filtration process can be seen in figure 3.21 below.

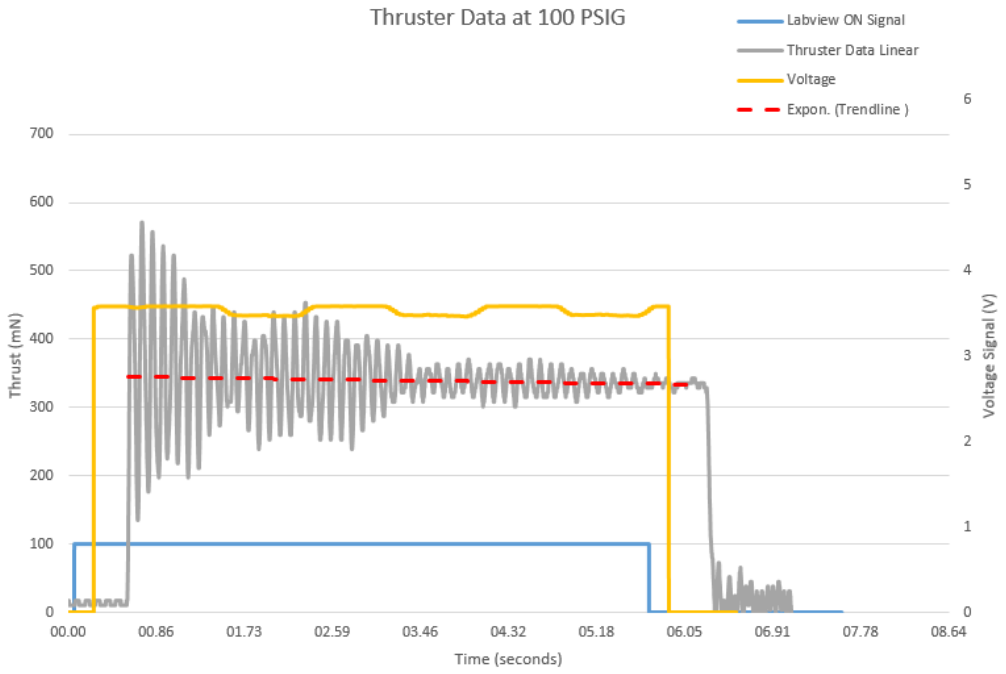

Figure 3.20: Engine Testing Results with Unfiltered Thrust Measurement

The results from nozzle thrust verification testing yielded an average force output of 363 mN with a peak thrust measurements 426mN. The response time of the engine was determined to be 38 milliseconds. The response time of the engine is considered from valve signal activation to the first thrust measurement peak. Figure 3.20, above, demonstrates the time variants between signal input, valve response and thrust.

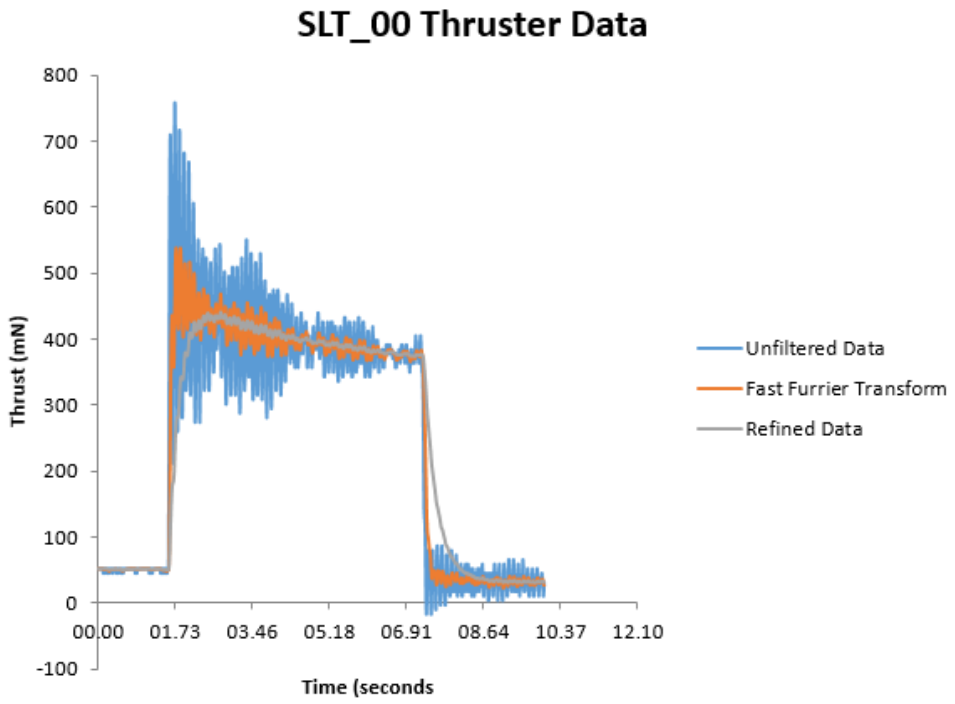

Figure 3.21: Data Filtration

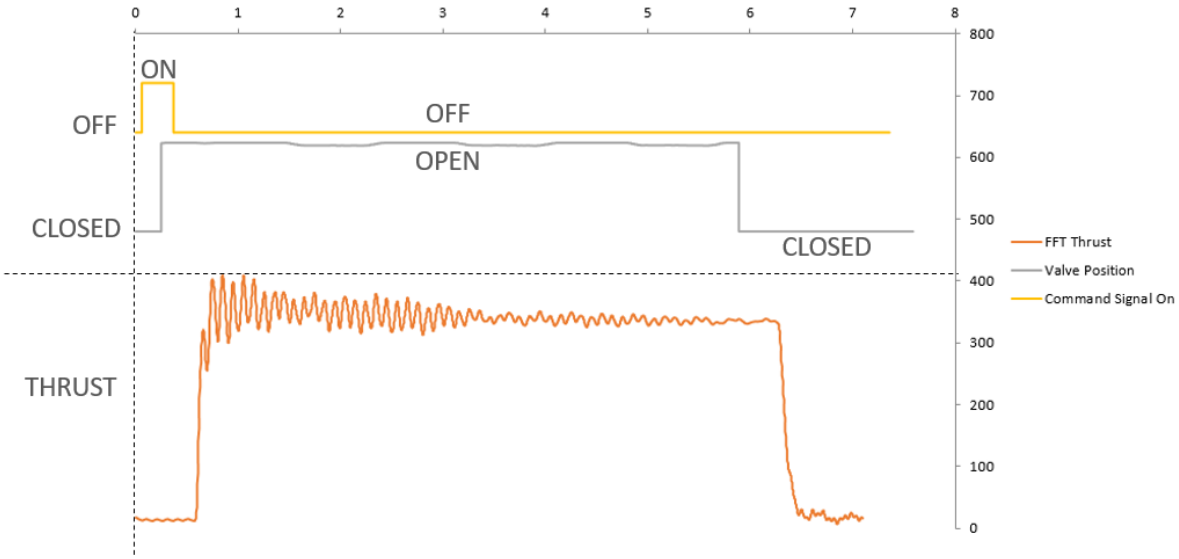

Figure 3.22: Engine Response

SECTION 3.3: PROPELLANT TANK

A propellant tank was designed based on NASA WSTF testing requirements alongside the needed pressure capabilities set by the chamber pressure for the cold gas nozzles. Testing requirements can be seen in table 3.4 below.

Table 3.5: Pressure Vessel Requirements

	Requirements	Pass/ Fail Criteria
1	Design will include integrated chassis to maximize available space	Inspection
2	Capable of holding an operating pressure with out fracture	100 psi
3	Burst pressure will be at least 4x greater than operating pressure	400 psi
4	Tank capacity should provide a theoretical minimum of 90 seconds of constant thrust	0.2-0.5 N
5	Design must allow integration of cartridge heaters to offset evaporative cooling	Inspection
6	Design can be re-used with minimal leaks	0.1-0.2 sccs

The tank was designed to deliver pressures up to 150psig. According to Cal-Poly's CubeSat Specifications, the material used for the chassis and large satellite components should be made of Aluminum as to minimize debris during mission re-entry. Material selection process for the cold gas demonstrator analyzed varying Aluminum alloys and found that Aluminum 6061-t6 would be best for the purposes of this project. Aluminum 6061 weldability and hardenability were key factors in the selection of the pressure vessel material.

3.3.1 Tank Development Concept

Initial tank concepts included a wall thickness of 2.5mm with an internal volume of 216cc. Heat exchanger ports placed at the center of the tank act as support structures for the unconventional shape of the pressure vessel.

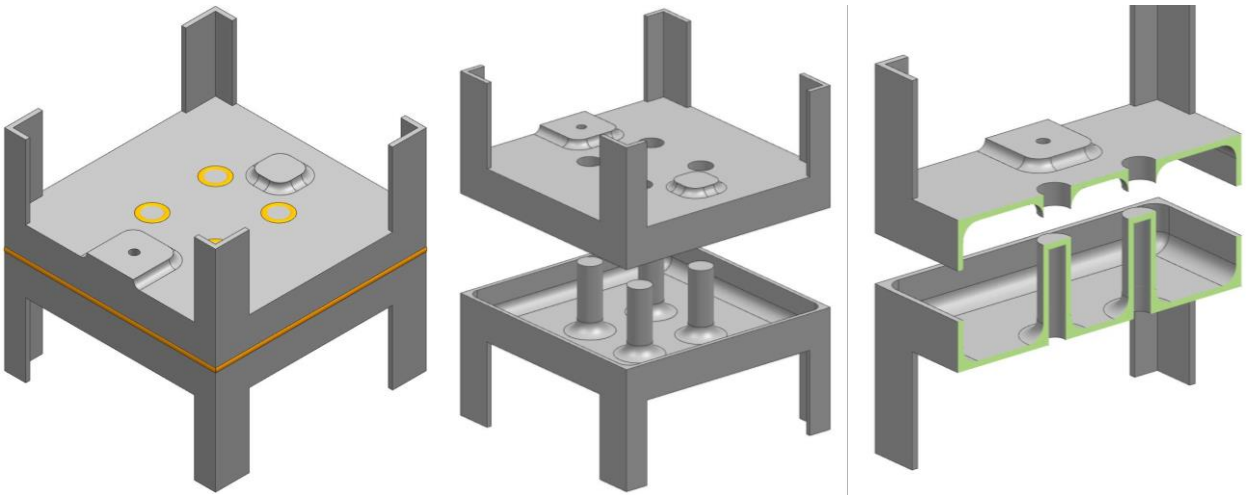

Figure 3.23: Consolidated Chassis and Pressure Vessel Concept

As mentioned previously, cylindrical and spherical designs are commonly used in the design of pressure vessels. Circular faces reduce the stresses during bending. Although these vessel formats are by far stronger than squared pressure vessels, the volume distribution can be awkward to integrate into a confined space. Although unconventional, a square pressure vessel allows maximum storage of the propellant in a thin and evenly distributed space. To compensate for the weaker internal structure, support beams were added to the interior of the tank to reduce stresses inside. The consolidated chassis also allows ease of integration for electrical and communication components, as these components follow standard dimensions. The internal tank volume is 230 cubic centimeters. Extruded bosses on the exterior provide increased thickness for the attachment of both plumbing and instrumentation. Central posts provide structural support and space for cartridge heaters.

Stress analysis on the pressure vessel conceptual design showed that there were high stress concentrations occurring at weld ports and alongside the body of the tank. Analysis iterations at increased pressures found a burst pressure to be approximately 500psi. The analysis included thermal stress concentrations at 0C and 100C, demonstrating the pressure vessel to have a minimum safety factor of 1.8 at 100C. At this pressure, stress concentrations will approach 300MPa, inducing failure at the heater post welds as seen in figure 3.24 below.

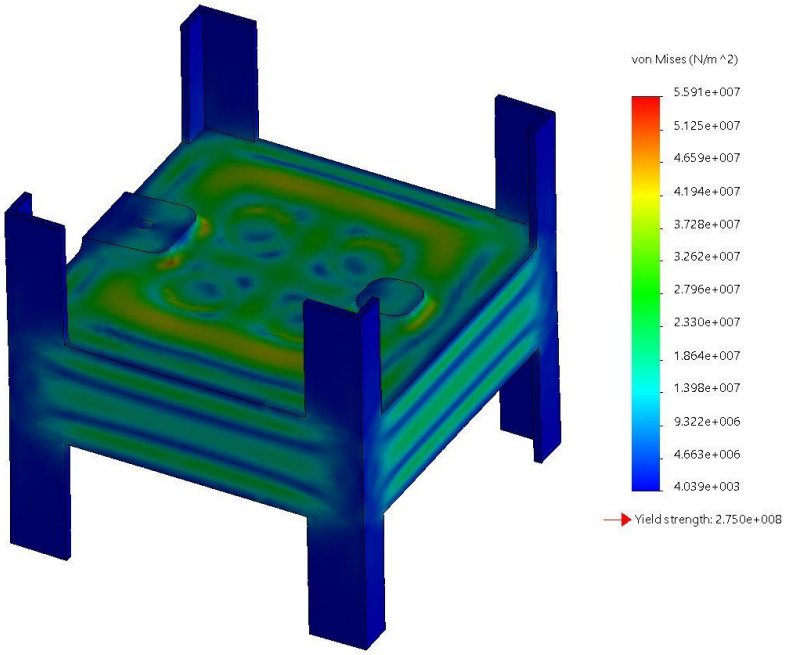

Figure 3.24: Stress Analysis of conceptual pressure vessel design

The stress analysis on the tank revealed that the primary sources of failure for the tank are found at the weld locations. Thermal stresses from welding degrade Aluminum 6061 to a toughness level of T-2. Solution treatment and metal aging methods increase the strength of the aluminum from the degraded toughness level T-2 to a toughness level of T-6. Solution treatment of Aluminum 6061is done by heating the pressure vessel to 400 C then quenching the metal in

room temperature water. Similarly aging of the metal is performed by heating vessel to 125 C for 24 hours and allowing it to cool down naturally to ambient conditions.

During pressure vessel heat treatment tank welds were exposed to thermal changes that showed fragility of welds along the centerline of tank. During this process hair line fractures and large cracks formed along the center weld of the pressure vessel. Weld failure is believed to have happened during the quenching process in solution treatment. Figure 3.25 demonstrates the weld fracture on the pressure vessel after quenching.

Figure 3.25: Weld fracture of pressure vessel

The original pressure vessel prototype was boded using laser welding with Aluminum 6061 beading. The failure of the tank is thought to be linked to the weld penetration. Laser welding is commonly used for welding of metals with low melting points such as Aluminum since welding elements requires lower temperatures and often are ideal to minimize thermal stresses and bending. These lower temperatures, however, prevent the welding material from fully penetrating walls thicker than 1.5mm (in the case of Aluminum). The bead weld thickness of the prototype pressure vessel was found to be about 1mm. Analyzing the results of the failed tank welds, future tank designs consider beveled butt welds for a stronger weld bond with full weld penetration along the

vessel walls. Butt welds require high temperature welding elements that can cause warping of the vessel walls.

3.3.2 Final Tank Design

Iterations of the pressure vessel considered the thermal stresses caused during welding and determined the new wall thickness to be 3.6mm. Aluminum 6061-T6 propellant tank has a total mass of 0.45 kg with storage volume of 216 cubic centimeters. The pressure vessel includes 2mm thick internal support structures intended to hold the heating elements to warm up the propellant to test conditions. These support structures lower stress at concentration areas above 300 MPa to near 100MPa. Final tank design can be seen in figure 3.26 and 3.27 below.

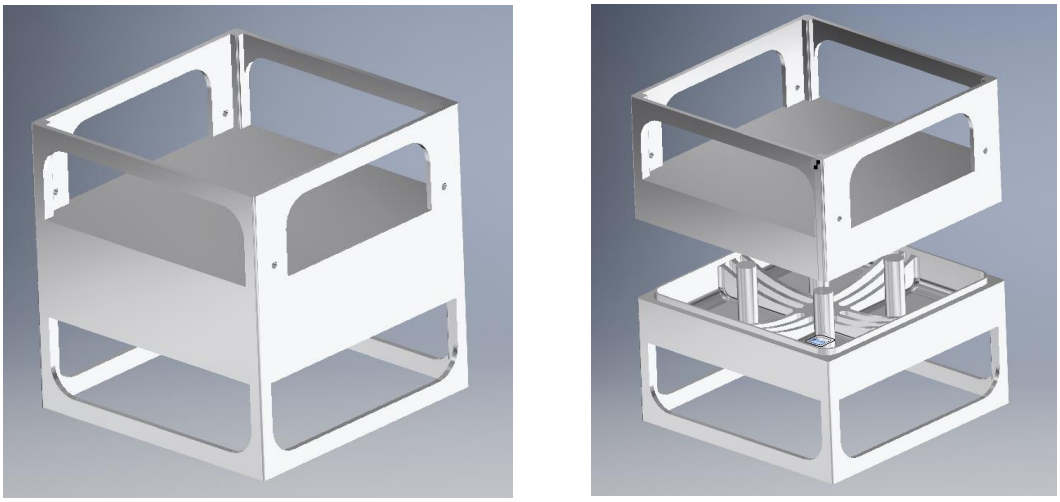

Figure 3.26: Final Pressure Vessel Design

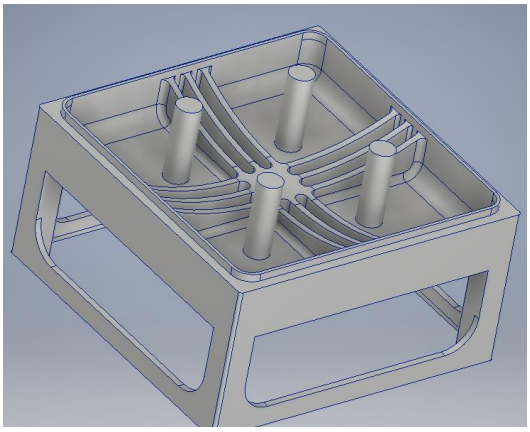

Figure 3.27: Pressure Vessel Internal Support Structure

Stress Analysis

A stress analysis was performed on the final concept for the pressure vessel. The results from this analysis can be seen in figures 3.28-3.29. The stress analysis was a two-part analysis meant to verify the structural integrity of the internal structures. The support beams visible in figure 3.28 are integral parts to the pressure vessel construction. Single Side Simulation Results at 300 psi yielded a maximum Von Mises Stress of 103 MPa, maximum displacement: 0.067 mm and minimum Safety Factor of 2.66.

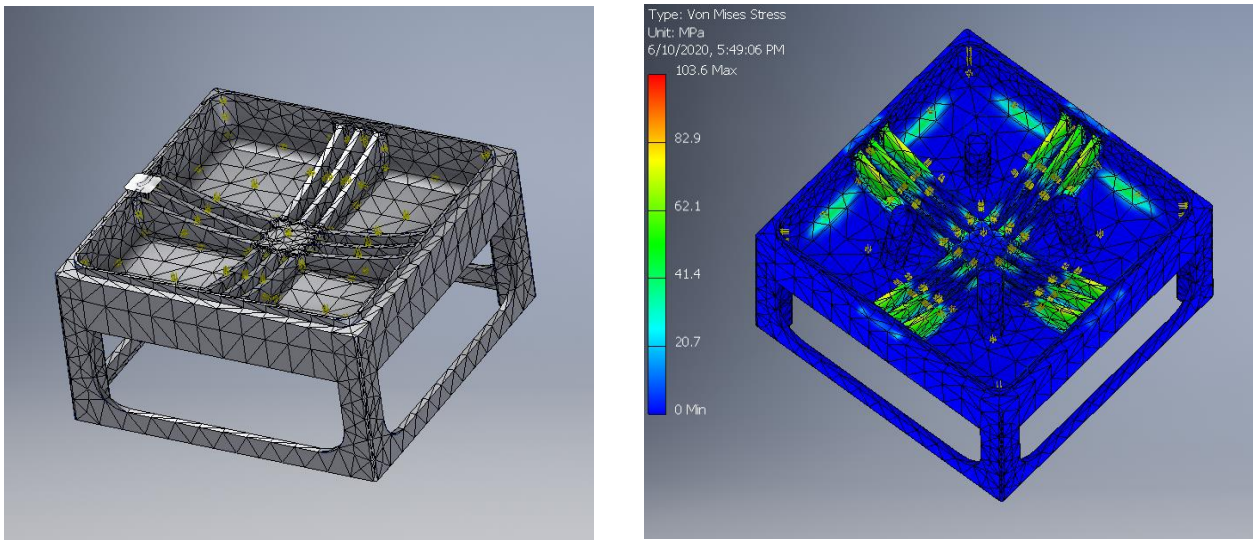

Figure 3.28: Stress Analysis of Internal Beam Structures

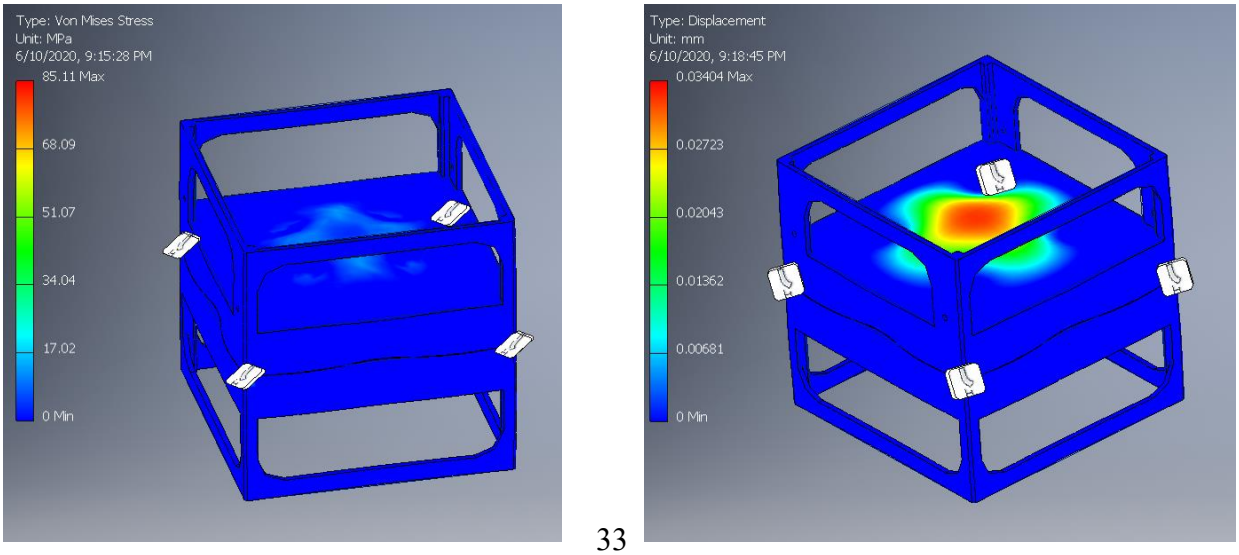

Figure 3.29: Pressure Vessel Stress Analysis

Chapter 4: Summary

Design, production and testing of the test components and instrument analysis tools were performed. Valve characterization and thruster testing for future work can be performed using the systems and proceed to be used for future testing of the cold gas demonstrator propulsion components.

The following goals were achieved by this work:

• Overall design configuration for testing and characterization of the miniature solenoid valves. Results found that with use of refrigerant 134a the pressure drop across the miniature solenoid valve to be 30-55 psig at a pressure inlet rage of 100-170psig. Results revealed that heat losses along the delivery feed system greatly impact the flow of the propellant and should be taken into consideration during system integration.

• A LabVIEW interface was created to control the different electrical components of the feed line system. The LabVIEW can record information every 3 microseconds.

• Design of a refrigerant recapturing system, purging system and vacuum system were all created for the system as well.

• Safety guidelines were created for the testing personnel.

• Calibration and instruction manual for the torsional thrust stand and laser measuring system.

• Testing of micro thrusters in preparation of propulsion system integration. The cold gas engine was found to deliver an average force of 363mN at an inlet pressure of 100psig. The response time of the system was measured to be 38 microseconds.

References

[1] Lan, Wenschel, Jonathan Brown, Armen Toorian, Roland Coelbo, Lori Brooks, Jordi Puig-Suari, and Robert Twiggs. "CubeSat development in education and into industry." In Space 2006, p. 7296. 2006.

[2] Deepak, Ravi A., and Robert J. Twiggs. "Thinking out of the box: Space science beyond the CubeSat." Journal of Small Satellites 1, no. 1 (2012): 3-7.

[3] Kulu, E. Nanosatellite & CubeSat Database. 2019. Available online: http://www.nanosats.eu/ (accessed on 27 April 2019).

[4] Zaberchik, Michael, Dan R. Lev, Eviatar Edlerman, and Avner Kaidar. "Fabrication and Testing of the Cold Gas Propulsion System Flight Unit for the Adelis-SAMSON Nano-Satellites." Aerospace 6, no. 8 (2019): 91.

[5] Ranjan, R., K. Karthikeyan, F. Riaz, and S. K. Chou. "Cold gas propulsion microthruster for feed gas utilization in micro satellites." Applied Energy 220 (2018): 921-933.

[6] Hinkley, D. (2008). A novel cold gas propulsion system for nanosatellites and picosatellites.

[7] Hashem, A. A. (2004). Design and testing of a cold gas system. ESASP, 555, 86-1.

[8] Camacho Lopez, Diana C., "Testing and Characterization of a Miniature Solenoid Valve for a Cold Gas propulsion System of a 1U CubeSat Demonstrator" (2019). Open Access Theses & Dissertations. 2832.

[9] Mehrparvar, A., Pignatelli, D., Carnahan, J., Munakat, R., Lan, W., Toorian, A., ... & Lee, S. (2014). Cubesat design specification rev. 13. The CubeSat Program, Cal Poly San Luis Obispo, US, 1(2).

[10] Imken, Travis K., Terry H. Stevenson, and E. Glenn Lightsey. "Design and testing of a cold gas thruster for an interplanetary CubeSat mission." Journal of Small Satellites 4, no. 2 (2015): 371-386.

Appendix A

$$\frac{A_e}{A_0} = \frac{\frac{\pi}{4}d_e^2}{\frac{\pi}{4}d_0^2} = \frac{(1.76 \cdot 10^{-3})^2}{(0.79 \cdot 10^{-3})^2} = 5$$

$$A_e = \frac{\pi}{4}d_e^2 = 1.267 \times 10^{-6} m^2$$

$$A_0 = \frac{\pi}{4}d_0^2 = 0.49017 \times 10^{-6} m^2$$

Specific Heat Ratio	1.108
Ideal Gas Constant	81.49 J/kgK
Saturation Pressure	665.8kPa
Atmospheric Pressure	~300 Pa
Fluid Temperature at Chamber	298K

IDEAL CONDITIONS

Mass Flow

$$\dot{m} = \frac{A_0 P_t}{\sqrt{T_t}} \sqrt{\frac{k}{R}} \left(\frac{k+1}{2}\right)^{-\frac{k+1}{2(k-1)}}$$

$$\dot{m} = \frac{0.49017 \times 10^{-6} \cdot 665800}{\sqrt{298}} \sqrt{\frac{1.108}{81.49}} \left(\frac{1.108+1}{2}\right)^{-\frac{1.108+1}{2(1.108-1)}}$$

$$\dot{m} = 1.3194 \times 10^{-3} \frac{kg}{s}$$

Exit Mach & Velocity

$$\frac{A_e}{A_0} = \left(\frac{k+1}{2}\right)^{-\frac{k+1}{2(k-1)}} \cdot \frac{\left(1+\frac{k-1}{2} \cdot M_e^2\right)^{\frac{k+1}{2(k-1)}}}{M_e}$$

$$\frac{A_e}{A_0} = \left(\frac{1.108+1}{2}\right)^{-\frac{1.108+1}{2(1.108-1)}} \cdot \frac{\left(1+\frac{1.108-1}{2} \cdot M_e^2\right)^{\frac{1.108+1}{2(1.108-1)}}}{M_e}$$

Solved using MatLab:

```
me = sym('me');
mach = secrat == ((k+1)/2)^(-(k+1)/(2*(k-1)))*(1+(k-
1)/2*me^2)^((k+1)/(2*(k-1)))/me;
Me=vpasolve(mach,me,[1,10]);
Me = ChokedMachNumber(100,1.108);

Me =
4.211428717147468635197194964902
```

$$\frac{T_e}{T_t} = \left(1 + \frac{k-1}{2} \cdot M_e^2\right)^{-1}$$
$$T_e = 298\left(1 + \frac{1.108-1}{2} \cdot 4.2114^2\right)^{-1}$$
$$\underline{T_e = 152.22K}$$
$$V_e = M_e\sqrt{k \cdot R \cdot T_e}$$
$$V_e = 4.2114\sqrt{1.108 \cdot 81.49 \cdot 152.22}$$
$$\underline{V_e = 493.72\frac{m}{s}}$$

Exit Pressure

$$\frac{P_e}{P_t} = \left(1 + \frac{k-1}{2}M_e^2\right)^{-\frac{k}{k-1}}$$
$$P_e = 665800\left(1 + \frac{1.108-1}{2} \cdot 4.2114^2\right)^{-\frac{1.108}{1.108-1}}$$
$$\underline{P_e = 676.33\ Pa}$$

Thrust

$$F = \dot{m} \cdot V_e + (P_e - P_\infty)A_e$$
$$F = 1.3194 \times 10^{-3} \cdot 493.72 + (676.33 - 300) \cdot 49.017 \times 10^{-6}$$
$$\underline{F = 669mN}$$

FABENS TEST CONDITIONS

Specific Heat Ratio	1.108
Ideal Gas Constant	81.49 J/kgK
Saturation Pressure	488.5 kPa
Atmospheric Pressure	~300 Pa
Fluid Temperature at Chamber	283K

Mass Flow

$$\dot{m} = \frac{A_0 P_t}{\sqrt{T_t}}\sqrt{\frac{k}{R}}\left(\frac{k+1}{2}\right)^{-\frac{k+1}{2(k-1)}}$$
$$\dot{m} = \frac{0.49017\times10^{-6}\cdot 488500}{\sqrt{283}}\sqrt{\frac{1.108}{81.49}}\left(\frac{1.108+1}{2}\right)^{-\frac{1.108+1}{2(1.108-1)}}$$
$$\underline{\dot{m} = 1.4 \times 10^{-3}\frac{kg}{s}}$$

Exit Mach & Velocity

$$\frac{A_e}{A_0} = \left(\frac{k+1}{2}\right)^{-\frac{k+1}{2(k-1)}} \cdot \frac{\left(1+\frac{k-1}{2}\cdot M_e^2\right)^{\frac{k+1}{2(k-1)}}}{M_e}$$

$$\frac{A_e}{A_0} = \left(\frac{1.108+1}{2}\right)^{-\frac{1.108+1}{2(1.108-1)}} \cdot \frac{\left(1+\frac{1.108-1}{2}\cdot M_e^2\right)^{\frac{1.108+1}{2(1.108-1)}}}{M_e}$$

Solved using MatLab:

```
me = sym('me');
mach = secrat == ((k+1)/2)^(-(k+1)/(2*(k-1)))*(1+(k-
1)/2*me^2)^((k+1)/(2*(k-1)))/me;
Me=vpasolve(mach,me,[1,10]);
Me = ChokedMachNumber(100,1.108);

Me =2.165
```

$$\frac{T_e}{T_t} = \left(1 + \frac{k-1}{2}\cdot M_e^2\right)^{-1}$$

$$T_e = 298\left(1 + \frac{1.108-1}{2}\cdot 2.165^2\right)^{-1}$$

$$\underline{T_e = 225K}$$

$$V_e = M_e\sqrt{k \cdot R \cdot T_e}$$

$$V_e = 2.165\sqrt{1.108 \cdot 81.49 \cdot 225}$$

$$\underline{V_e = 309.15\frac{m}{s}}$$

Exit Pressure

$$\frac{P_e}{P_t} = \left(1 + \frac{k-1}{2}M_e^2\right)^{-\frac{k}{k-1}}$$

$$P_e = 488500\left(1 + \frac{1.108-1}{2}\cdot 2.625^2\right)^{-\frac{1.108}{1.108-1}}$$

$$\underline{P_e = 47912\ Pa}$$

Thrust

$$F = \dot{m}\cdot V_e + (P_e - P_\infty)A_e$$

$$F = 1.4\times 10^{-3}\cdot 358.2 + (47912 - 300)\cdot 1.267\times 10^{-6}$$

$$\underline{F = 493mN}$$

EXPECTED WSTF TESTING CONDITIONS

Specific Heat Ratio	1.108
Ideal Gas Constant	81.49 J/kgK
Saturation Pressure (tank pressure)	2169kPa
Atmospheric Pressure	~300 Pa
Tank Temperature	344K

Mass Flow

$$\dot{m} = \frac{A_0 P_t}{\sqrt{T_t}} \sqrt{\frac{k}{R}} \left(\frac{k+1}{2}\right)^{-\frac{k+1}{2(k-1)}}$$

$$\dot{m} = \frac{0.49017\times10^{-6}\cdot 2169000}{\sqrt{344}} \sqrt{\frac{1.108}{81.49}} \left(\frac{1.108+1}{2}\right)^{-\frac{1.108+1}{2(1.108-1)}}$$

$$\underline{\dot{m} = 1.27 \times 10^{-3}\ \frac{kg}{s}}$$

Exit Mach & Velocity

$$\frac{A_e}{A_0} = \left(\frac{k+1}{2}\right)^{-\frac{k+1}{2(k-1)}} \cdot \frac{\left(1+\frac{k-1}{2}\cdot M_e^2\right)^{\frac{k+1}{2(k-1)}}}{M_e}$$

$$\frac{A_e}{A_0} = \left(\frac{1.108+1}{2}\right)^{-\frac{1.108+1}{2(1.108-1)}} \cdot \frac{\left(1+\frac{1.108-1}{2}\cdot M_e^2\right)^{\frac{1.108+1}{2(1.108-1)}}}{M_e}$$

Solved using MatLab:

```
me = sym('me');
mach = secrat == ((k+1)/2)^(-(k+1)/(2*(k-1)))*(1+(k-
1)/2*me^2)^((k+1)/(2*(k-1)))/me;
Me=vpasolve(mach,me,[1,10]);
Me = ChokedMachNumber(100,1.108);

Me = 2.625
```

$$\frac{T_e}{T_t} = \left(1 + \frac{k-1}{2}\cdot M_e^2\right)^{-1}$$

$$T_e = 344\left(1 + \frac{1.108-1}{2}\cdot 2.625^2\right)^{-1}$$

$$\underline{T_e = 250.71K}$$

$$V_e = M_e\sqrt{k\cdot R\cdot T_e}$$

$$V_e = 2.625\sqrt{1.108\cdot 81.49\cdot 250.71}$$

$$\underline{V_e = 394.9\frac{m}{s}}$$

Exit Pressure

$$\frac{P_e}{P_t} = \left(1 + \frac{k-1}{2} M_e^2\right)^{-\frac{k}{k-1}}$$

$$P_e = 2169000 \left(1 + \frac{1.108-1}{2} \cdot 2.625^2\right)^{-\frac{1.108}{1.108-1}}$$

$$\underline{P_e = 85697\ Pa}$$

Thrust

$$F = \dot{m} \cdot V_e + (P_e - P_\infty) A_e$$

$$F = 1.27 \times 10^{-3} \cdot 394.9 + (85697 - 300) \cdot 1.76 \times 10^{-6}$$

$$\underline{F = 610mN}$$

Vita

Norma Perea attended the University of Texas at El Paso seeking Bachelor's in Mechanical Engineering after accepting the Presidential Scholarship, the Texas Grant, and the Pell Grant. During her time as an undergraduate student she was given the opportunity to work at the Center for Space Exploration Technology as a Mechanical Engineering undergraduate research assistant for Department of Defense Hybrid propulsion program under the supervision of Dr. Norman Love. She received her bachelor's in mechanical engineering from UTEP in 2016. She was accepted into the Master of Science in Mechanical Engineering program where she continued her work with cSETR as a graduate research assistant under the guidance of Dr. Joel Quintana, leading the Cold Gas Demonstrator project, a collaboration with NASA White Sands Test Facility to test the capabilities of a magnetic levitation table. During her time in UTEP, Norma has interned at NASA Glenn Research Center and Lockheed Martin Space. She has published at Southwest Emerging Technologies in 2018 and 2020 and AIAA Jet Propulsion Conference in 2020.

Contact Information: norma_perea64@yahoo.com